

Extended comment on *Nature* 586, 373 (2020) by E. Snider *et al.*

D. van der Marel¹ and J. E. Hirsch²

¹*Department of Quantum Matter Physics, University of Geneva, 24 Quai Ernest-Ansermet, 1211 Geneva, Switzerland*

²*Department of Physics, University of California, San Diego, La Jolla, CA 92093-0319, USA*

In Ref. [1] Snider *et al.* reported room temperature superconductivity in carbonaceous sulfur hydride (CSH) under high pressure. Recently the data for the temperature dependent ac magnetic susceptibility presented in figures of Ref. [1] (labeled “superconducting signal” by the authors) for 6 different pressures, as well as the corresponding raw data (labeled “measured voltage” by the authors) have appeared in the form of tables [2]. Here we analyze the “superconducting signal” as well as the corresponding raw data for all 6 pressures. We find that (i) the “superconducting signal” can be described as the superposition of a smooth curve and a quantized component, which for 5 pressures was smoothed using the adjacent averaging method, and for one pressure (160 GPa) was not smoothed. We introduce a correlation method to detect a small signal buried in a noisy background. We apply this method to the raw data and show for two pressures that the raw data are the superposition of the “superconducting signal” (characterized by the aforementioned features) and a “background signal” containing noise. For the other pressures the noise amplitude of the raw data is too large to provide a statistically significant signature of this type.

I. INTRODUCTION

In Ref. [1] it is reported that a material termed carbonaceous sulfur hydride (hereafter called CSH) is a room temperature superconductor. Data for resistance versus temperature and ac susceptibility versus temperature at six different pressures show drops suggesting superconducting transitions. Recently two of the authors of Ref. [1] have posted the numerical values of the data for the ac susceptibility curves presented in Ref. [1], as well as the underlying raw data, on arXiv [2]. The raw data and the data presented in Ref. [1] are called “measured voltage” and “superconducting signal” respectively in Ref. [2]. Here we give an analysis of the ac susceptibility data for all pressures. We begin with the “superconducting signal” and the “measured voltage” at $p = 160$ GPa. Next the “superconducting signal” and the “measured voltage” for all other pressures are analyzed. Other analysis of the susceptibility data in Ref. [2] were presented in Refs. [3–5].

II. ANALYSIS OF THE 160 GPa DATA

Fig. 1a shows the susceptibility corresponding to pressure 160 GPa shown in Extended Data Figure 7d of Ref. [1]. The numerical values are given in the second column of Table 5 of Ref. [2] (labeled “superconducting signal”). A superconducting transition appears to take place around $T = 170$ K. In Fig. 1 panels c and d these data are shown on a 15 times expanded y-axis. Because of the steep rise at 170 K the regions above and below 170 K need to be displayed in separate panels. A similar zoom of the 160 GPa curve was previously shown in Fig. 9 of Ref. [5]. One of the striking features is a series of discontinuous steps. These steps are directly visible to the eye in the temperature ranges where $\chi'(T)$ has a weak temperature dependence. However, they are also present in the range where $\chi'(T)$ rises steeply as a function of temperature, as can be seen by calculating the

difference between neighboring points

$$\Delta\chi(j) = \chi(T_j) - \chi(T_{j-1}). \quad (1)$$

This quantity, shown in Fig. 1 b, exhibits an intriguing “aliasing” effect in the “shadow curves” displaced vertically by integer multiples of 0.1655 (in section V this will be refined to 0.16555 ± 0.00005 by examining the noise of the 3d and 4th derivatives). To make this crisp, the vertical axis of Fig. 1 b corresponds to $\Delta\chi(j)/0.1655$. Clearly this is a set of curves vertically offset by an integer $n = -1, 0, 1, 2, 3$ and 4. The most systematic offsets in sign and size occur between 169.6 K and 170.1 K.

By shifting continuous segments of the curves by an amount $0.16555n$, with n integers that can be read off from Fig. 1b, it is a simple and straightforward task to ‘unwrap’ the vertical offsets [6]. The result for the two separate ranges above and below 170 K is displayed in Fig. 1 e and f, and for the full range in panel g. Comparing panel e to c, and f to d it is possible to verify that the resulting curves are extremely smooth and completely free of discontinuities. Comparing panel g to a the steep rise at 170 K is absent from panel g. As a consistency check $\Delta\chi(j)$ of panel g was finally calculated and is shown in panel h. Comparing the result shown in panel h with that in panel b (shown with the same vertical scale to facilitate comparison) it can be seen that there are no shadow curves in panel h, demonstrating that not only the temperature dependence of panel g is smooth, the differential shown in panel h is, surprisingly for an experimental quantity, also completely smooth.

The behavior of the data shown in Fig. 1 c and d, together with the fact that the segments can be joined by vertical shifts that are all of the same form $0.16555n$, indicates that the disconnected segments are portions of a continuous curve that has been broken up by quantized steps. The sequence of steps form together a quantized component which is entirely responsible for the steep rise of $\chi'(T)$ at 170 K seen in Fig. 1 a. The data (superconducting signal)

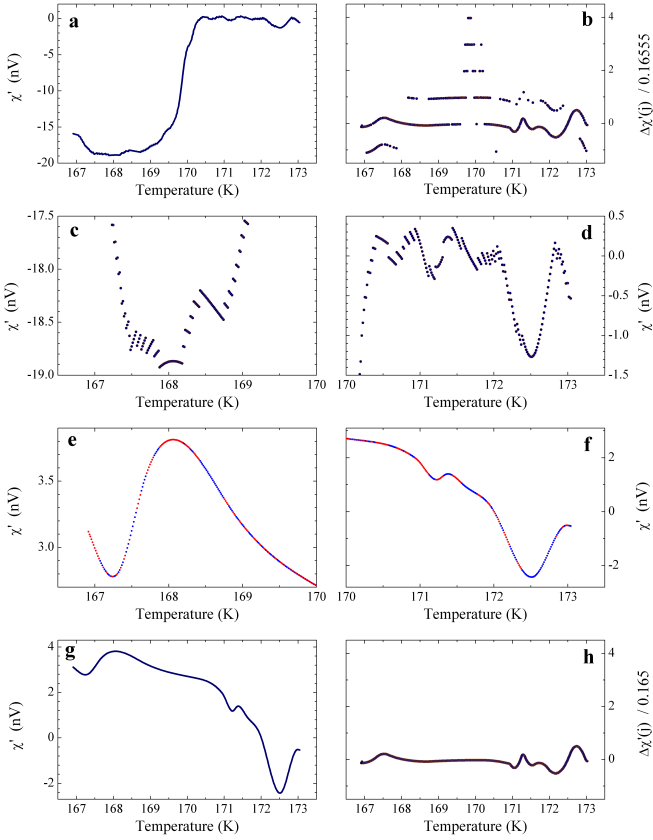


FIG. 1. **a**, Susceptibility data (“superconducting signal”) for CSH at pressure 160 GPa, from the numerical data of Table 5 of Ref. [2]. **b**, The difference between neighboring points of panel **a** divided by 0.16555. **c** and **d**, The data of panel **a** on an enlarged scale. **e**, **f** and **g**, The data of panels **c**, **d** and **a** after unwrapping with integer multiples of 0.16555. The different colors of panels **e** and **f** refer to disconnected segments of panels **c** and **d**. **h**, Same as panel **b** but now using the unwrapped data of panel **g**. The same vertical scale is used as for panel **b**.

of Fig. 1 **a** can be expressed as:

$$\text{Superconducting Signal} = \text{quantized component} + \text{unwrapped curve} \quad (2)$$

where the unwrapped curve is given in Fig. 1 **g**. Fig. 2 shows the same information as panels **a-d** of Fig. 1 for the quantized component. The connected segments are now horizontal, and the y-values in panel **b** are integers.

According to Ref. [1], a background signal measured at 108 GPa was subtracted from the “measured voltage” in obtaining the published data (“superconducting signal”) in Ref. [1]. In other words,

$$\text{Superconducting Signal} = \text{Measured Voltage} - \text{Background Signal} \quad (3)$$

Comparison of Eq. (3) and Eq. (2) strongly suggests that the measured voltage and background signal in Eq. (3) correspond to the quantized component and $-1 \times$ unwrapped curve in Eq. (2) respectively.

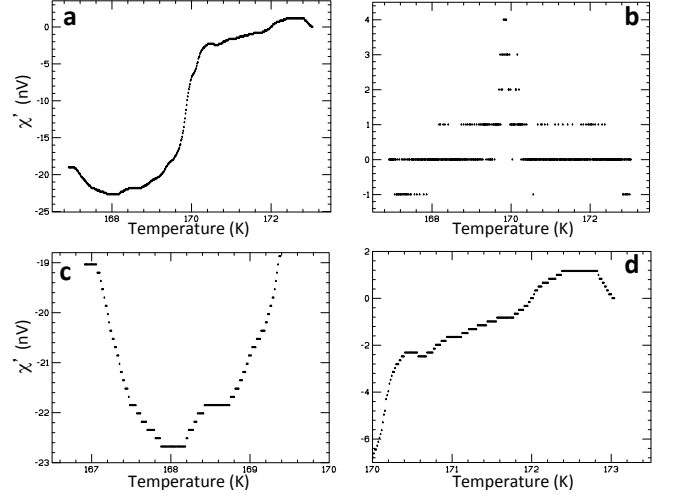


FIG. 2. **a**, Quantized component of susceptibility data (“superconducting signal”) for CSH at pressure 160 GPa. **b**, The difference between neighboring points of panel **a** divided by 0.16555. **c** and **d**, The data of panel **a** on an enlarged scale.

III. A POSSIBLE EXPLANATION OF THESE RESULTS?

To begin to understand these results we have to understand (a) why the measured voltage deduced in section II (quantized component) is a series of flat steps separated by jumps of a fixed magnitude 0.16555 nV, and (b) why the background signal deduced in section II (the negative of the unwrapped curve) is a smooth curve with no experimental noise.

(a) A digital lock-in amplifier will yield discrete values for the measured voltages, where the size of the step between neighboring values of measured voltages is given by the instrumental resolution. Given our conclusion in section II that the quantized component shown in Fig. 2a could be the raw data (measured voltage), this would indicate that the resolution of the instrument in this measurement was of order 0.2 nV. Such a low resolution could result from setting the digitizer range of the lock-in amplifier to a large value, approximately $100 \mu\text{V}$ [7].

(b) The smooth behavior of the background signal ($-1 \times$ panel **g** of Fig. 1) could be explained if, rather than measured values of the background signal, a polynomial fit to the measured values was subtracted from the raw data. However, Ref. [1] does not mention such a procedure.

IV. BACKGROUND SIGNAL AND MEASURED VOLTAGE

In the previous section we have concluded that a possible way to understand the very unusual nature of the susceptibility data for 160 GPa reported in Ref. [1] could be if the measured raw data are the quantized component of the superconducting signal shown in panel **a** of Fig. 2, and the background signal is given by the negative of the unwrapped curve panel **g** of Fig. 1. On the other hand, the

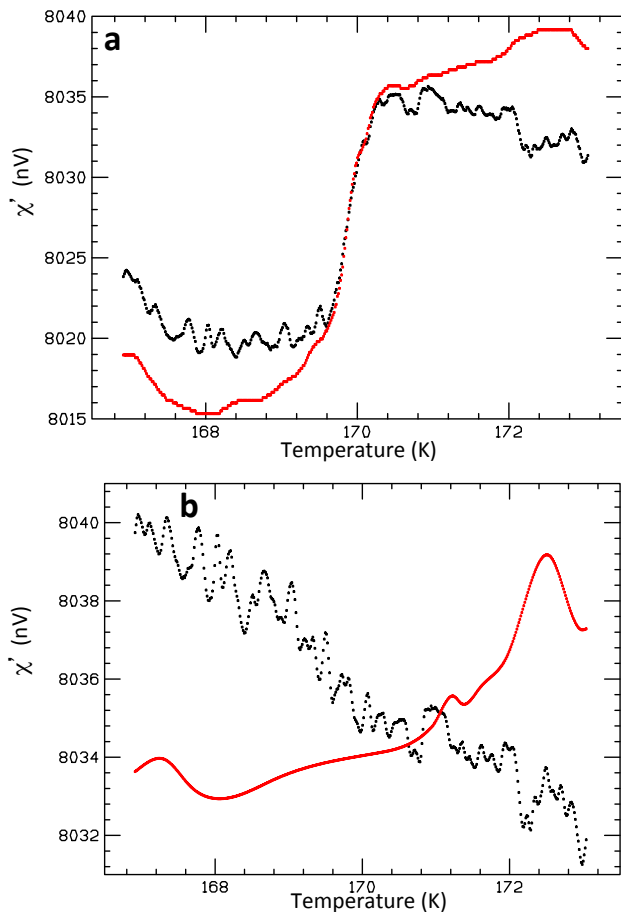


FIG. 3. **a**, “measured voltage” reported in Ref. [2] for 160 GPa (black points), compared with quantized component of susceptibility data (red points). **b**, Background signal inferred by subtraction of reported “measured voltage” and “superconducting signal” in Ref. [2] (black points), compared with background signal inferred from unwrapping of the susceptibility data (red points).

superconducting signal as well as the measured raw data were reported in Ref. [2] Table 5, and we can infer from them the background signal simply by subtraction.

Therefore, in Figs. 3 **a** and **b** we compare the reported raw data and the background signal inferred from the reported raw data and the reported data [2] with our hypothesized raw data and background signal deduced in section II.

It can be seen in Fig. 3 that there is a complete disconnect between the raw data and the background signal inferred from the numbers reported in Ref. [2], and the raw data and background signal inferred from the analysis of the superconducting signal [1] (numerical values given in Ref. [2]) discussed in section II. In particular, there is certainly no way that a polynomial fit of the black points in Fig. 3**b** would have any resemblance to the red curve shown in Fig. 3**b**, and there is a significant difference between the black and red curves in Fig. 3**a**.

There is also no quantization of measured voltages in the

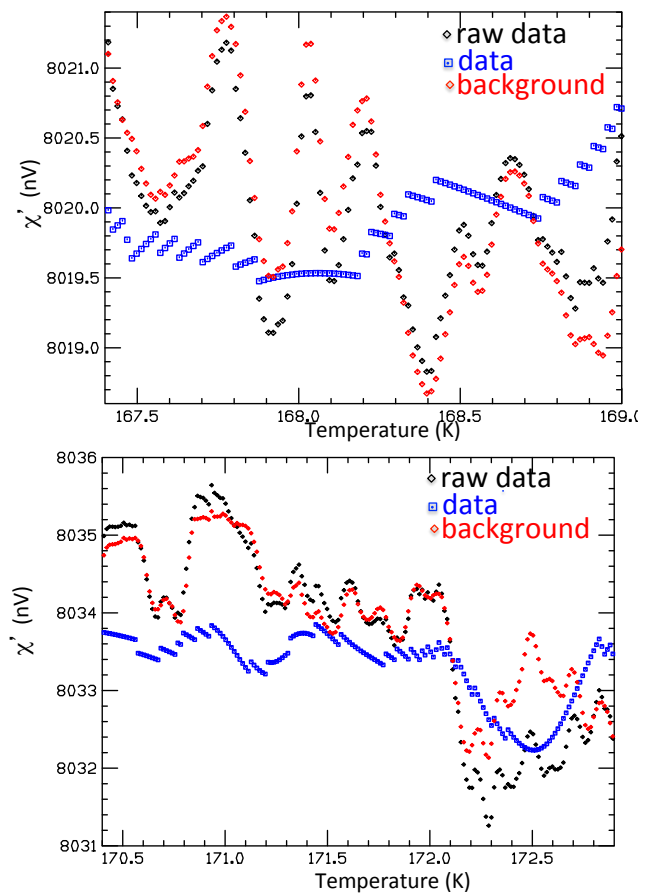


FIG. 4. Raw data, data and background signal inferred by subtraction, obtained from the numerical values reported in Table 5 of Ref. [2], for the low and high temperature regions of the 160 GPa data shown in panels **c** and **d** of Fig. 1 .

raw data reported in Ref. [2]. The reported measured values of the measured voltage are given in Table 5 of Ref. [2] with 11 significant digits. This is *not* necessarily the experimental resolution. The experimental resolution is set by the complete analogue and digital chain of which the DAC is the last element. The smallest step between neighboring temperatures in Table 5 of Ref. [2] is of order 0.0001 nV. Hence the resolution of the experimental setup is 0.0001 nV or a smaller number. This is about three orders of magnitude higher resolution than the resolution of the measuring device that would yield the quantized component (red curve in Fig. 3a) as measured raw data.

It can also be seen in Fig. 3 that there is much larger noise in the raw data and background signal reported in Ref. [2] than there is in the red curves that were deduced from the reported superconducting signal in section II. The fact that the reported superconducting signal is significantly less noisy than the reported raw data was already noted in Ref. [5], not only for pressure 160 GPa but for all other pressures as well. This is independent of the unwrapping analysis discussed in the earlier sections. In Fig. 4 we show the raw data, the data, and the background signal obtained

from the values reported in Table 5 of Ref. [2], for the low and high temperature parts of the 160 GPa data. It can be seen that in order for the data (blue points) to result from subtraction of a background (red points) from raw data (black points) the oscillations in the background signal, presumably arising from instrumental noise, have to closely track oscillations in the raw data. Independently measured raw data and background signal do not have that property.

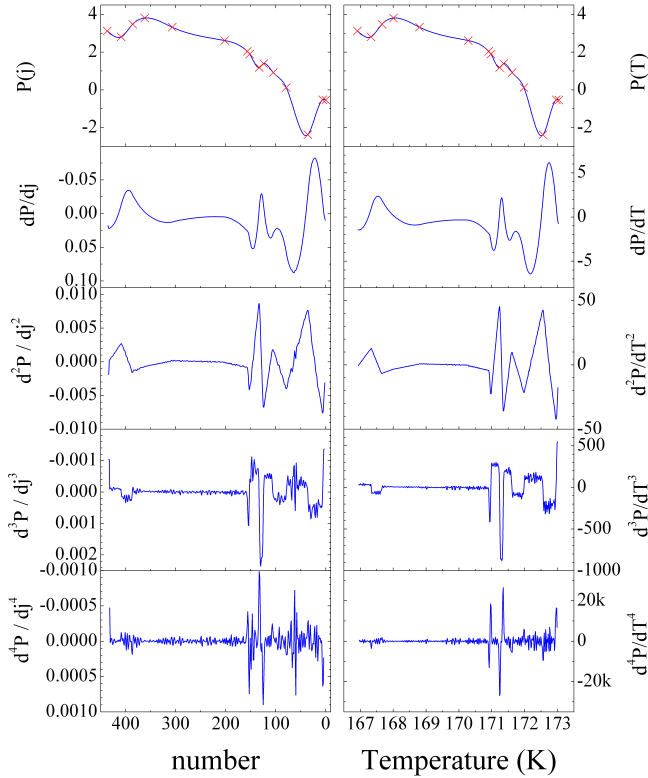


FIG. 5. From top to bottom: Unwrapped component of the susceptibility and its first, second, third and fourth derivatives. Left panels: Numerical derivatives with respect to the row number. Right panels: Numerical derivatives with respect to the temperature. The parts of the curves between neighboring red crosses in the top panels are described by third order polynomials (see text for explanation).

V. PROPERTIES OF THE UNWRAPPED CURVE

The remarkable smoothness of the unwrapped curve obtained through the analysis in section II is illustrated by Fig. 5 where this curve is displayed together with the first, second, third and fourth derivative. The n 'th derivative of the j 'th point were calculated by applying the linear regression expression [8] to the $n-1$ 'th derivatives at j and $j \pm 1$. Consequently the n 'th derivative can only be calculated for a smaller subset of points, namely $n \leq j \leq 437 - n$.

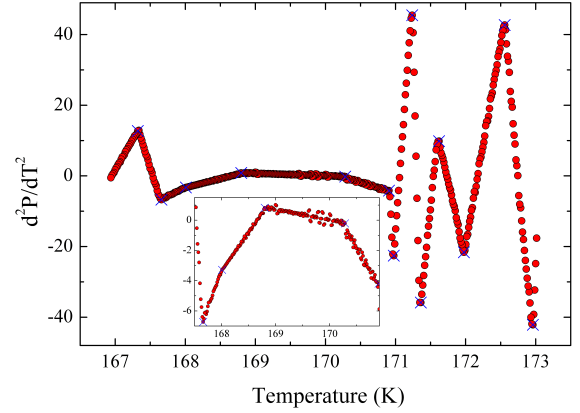


FIG. 6. Enlarged third right panel from the top of Fig. 5, showing the fourteen linear segments for the second derivative. The inset shows the center part enlarged further.

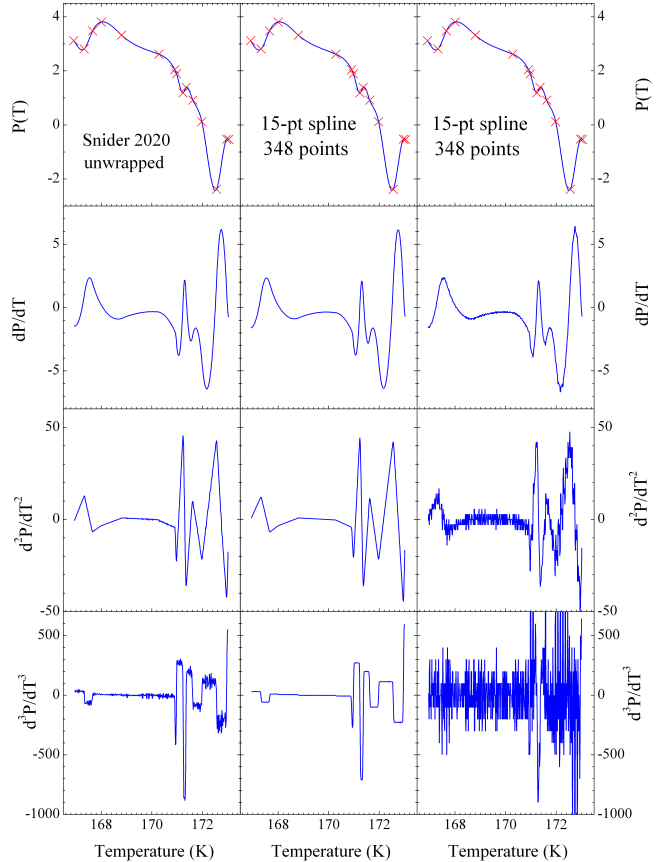


FIG. 7. Left from top to bottom : Unwrapped component of the susceptibility and its first, second, and third derivatives. Right (middle) from top to bottom : 15-node cubic spline with natural boundary conditions generated with an older (newer) version of commercial plotting software and its first, second, and third derivatives. The nodes are indicated as red crosses in the top panels.

segment	j_1	j_2	a	b	c	d
			nV	nVK ⁻¹	nVK ⁻²	nVK ⁻³
1	0	6	$-4.9708 \cdot 10^8$	$+8.61772 \cdot 10^6$	-49800.86194	+95.93123
2	6	36	$1.91612 \cdot 10^8$	$-3.32767 \cdot 10^6$	+19263.50719	-37.17133
3	36	79	$-7.45267 \cdot 10^7$	$+1.29874 \cdot 10^6$	-7544.15403	+14.60746
4	79	105	$7.3647 \cdot 10^7$	$-1.28653 \cdot 10^6$	+7491.41848	-14.54077
5	105	124	$-1.66029 \cdot 10^8$	$+2.90356 \cdot 10^6$	-16925.99285	+32.88943
6	124	133	$7.22616 \cdot 10^8$	$-1.26553 \cdot 10^7$	+73878.63337	-143.76142
7	133	152	$-2.28148 \cdot 10^8$	$+4.00122 \cdot 10^6$	-23390.90027	+45.58059
8	152	157	$3.8154 \cdot 10^8$	$-6.69719 \cdot 10^6$	+39185.38867	-76.42487
9	157	202	$4.9976 \cdot 10^6$	-88089.66243	+517.57022	-1.01366
10	202	307	565564.77819	-9977.32472	+58.67335	-0.11502
11	307	362	$-4.07314 \cdot 10^6$	+72452.65657	-429.58792	+0.84903
12	362	386	$-7.61789 \cdot 10^6$	+135753.45679	-806.38874	+1.59667
13	386	409	$4.96114 \cdot 10^7$	-888374.04134	+5302.58851	-10.55012
14	409	437	$-2.67393 \cdot 10^7$	+480488.75329	-2878.02049	+5.74622

TABLE I. Coefficients of the expression $\chi = a + bT_j + cT_j^2 + dT_j^3$ where T_j is the j 'th temperature for the 14 segments defined by $j_1 \leq j \leq j_2$. The coefficients were obtained by least square fitting the corresponding segments to a third order polynomial.

Only the fourth derivative is too noisy for readout. In the second derivative graph, shown in more detail in Fig. 6, all segments are straight lines. This clearly demonstrates that this curve is a chain of 14 polynomials of order 3. The curve, and its 1st, 2nd and 3rd derivatives fits the profile of a cubic spline [9] with 15 nodes. The nodes are shown as crosses in the top panels of Fig. 5 and in Fig. 6.

The temperatures are not equally spaced. To check whether the underlying functional dependence of the smooth curve is better described by temperature or by row number, the numerical derivatives with respect to T (right) are compared to those with respect to row number j (left) in Fig. 5. The noise level for third and fourth derivative in the right hand panel indicates that the 14 segments of the unwrapped curve are slightly less well described as functions of the row number than the temperature. The coefficients using the temperature representation are given in Table I. The noise level is the lowest for the offset in the range 0.16555 ± 0.00005 . Furthermore the 14 segments appear to be the output of a spline. The second derivatives extrapolate to zero at the extremal nodes, which corresponds to the so-called "normal" boundary conditions of the cubic spline [10] [11]. This is the standard spline option of commercial plotting software. Applying the cubic spline with natural boundary conditions of different versions of commercial plotting software to the 15 nodes, and exporting on the temperature range defined by the two extremal nodes, gives the result in the middle and righthand panels of Fig. 7. The smaller noise of the middle column as compared to the right hand column (especially the third derivative) signals an improvement over time of the spline accuracy in subsequent versions of this software.

VI. FIRST PROTOCOL

According to Ref. [1]: "The background signal, determined from a non-superconducting C-S-H sample at 108

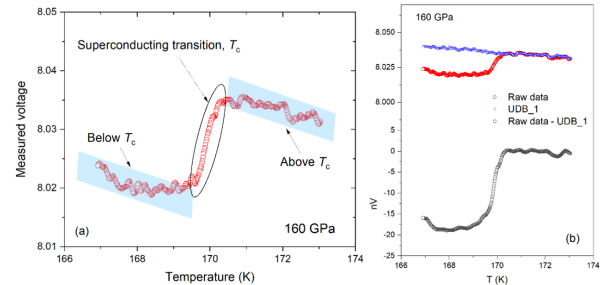


Fig. 2 AC susceptibility data. (a) Raw data measured at 160 GPa. The profile of the regions highlighted in blue are used as part of the UDB 1. (b) Measured voltage from the susceptibility measurement explained in experimental details section in Ref. 1 and 2 for 160 GPa. Raw data (red), UDB_1 (blue) and raw data - UDB_1 (black).

FIG. 8. Source: Fig. 2a of Ref. [12].

GPa, has been subtracted from the data". Later in Ref. [12]: "We note here that we did not use the measured voltage values of 108 GPa as the background. We use the temperature dependence of the measured voltage above and below the T_c of each pressure measurement and scale to determine a user defined background." The method illustrated in Fig. 2a of Ref. [12] is reproduced in Fig. 8. In particular it does *not* lead to the "superconducting signal" reported for 160 GPa, *i.e.* the superposition of a 15-node cubic spline and a quantized component. To introduce those two features in the "superconducting signal" requires that they are already present in the raw data, in the "user defined background", or in both.

It will become possible to address the issues raised in Ref. [12] after the authors release the numerical values for their UDB1 ("user defined background method 1") along with a detailed documentation of how this is derived -and can be reproduced by others- from the experimental data.

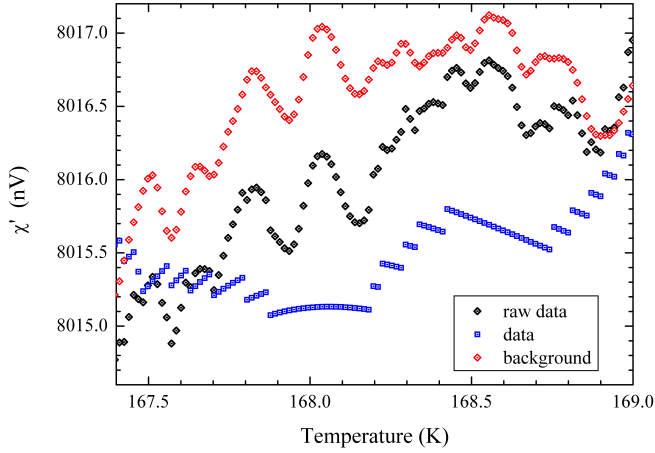


FIG. 9. Simulation of Eq. 4. Black: measured voltage. Red: Background Signal. Blue: superconducting signal.

VII. SECOND PROTOCOL

The inconsistencies pointed out in section VI do not occur when Eq. 3 is rearranged as follows [13]:

$$\text{Measured Voltage} = \text{Superconducting Signal} + \text{Background Signal} \quad (4)$$

This also removes the incongruences of the noise: The noise of “Measured Voltage” is now the sum of the noises of “superconducting signal” and “Background signal” and therefore bigger than the noise of each of the latter two. A simulation is shown in Fig. 9, where for the Background panel an arbitrary curve was taken having a noise structure similar to that shown in Fig. 2a of Ref. [12] (also shown in Fig. 3b). Globally the features of “measured voltage” (red symbols) are similar to those in Fig. 4 upper panel. Despite differences in the noise structure, points in common of Fig. 4 and Fig. 9 are that (i) the “measured voltage” is noisier than “superconducting signal” and “Background Signal” and (ii) several (but not all) of the steps present in the “superconducting signal” also show up in “measured voltage”. In Fig. 10 we show the raw data points corresponding to connected segments of the data points identified by color and joined. It is apparent that several of the jumps in the data points are reflected in the raw data. This indicates that whatever the explanation is for the existence of these jumps in the data points has to also account for their existence in the raw data.

VIII. “SUPERCONDUCTING SIGNAL” AT ALL PRESSURES

The data at 160 GPa stood out because of the striking sawtooth shape of the “superconducting signal”, which is in fact the superposition of a smooth curve composed of third order polynomials (15 point cubic spline with normal boundary conditions) and a quantized component in

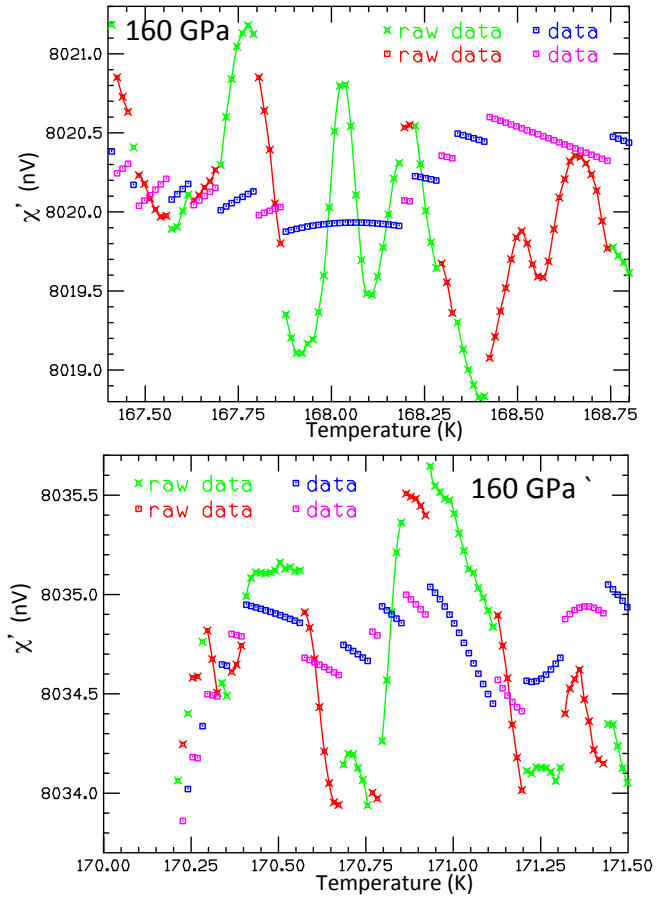


FIG. 10. “Measured voltage” (“raw data”) and “superconducting signal” (“data”) obtained from the numerical values reported in Table 5 of Ref. [2], for low and high temperature regions of the 160 GPa data. “Raw data” points corresponding to each of the connected segments of the “data” points are joined. The colors green and red for the “raw data” (“measured voltage”) points correspond to the colors blue and magenta for the “data” (“superconducting signal”) respectively.

increments of 0.1655 nV. For the other pressures the “superconducting signal” does not have the conspicuous sawtooth appearance. However, just like for 160 GPa the reported data [2] show much larger noise in the measured voltage and background signal than in the “superconducting signal” obtained by subtraction [3–5]. Here we show that this can be understood according to the “second protocol” discussed in the previous section, with one additional step.

From Figs. 17, 18, 19 showing the quantities obtained from [1, 2, 16]

$$\begin{aligned} \Delta\chi(j) &= \chi(j) - \chi(j-1) \\ \Delta^2\chi(j) &= \Delta\chi(j) - \Delta\chi(j-1) \end{aligned} \quad (5)$$

and Fig. 11 showing the distribution of $\Delta^2\chi$ in the form of histograms (this method was suggested by Dukwon [14, 15]), we see that for all pressures there are underlying steps present in the temperature traces. The size of the steps differs from one pressure to another. The quantization steps

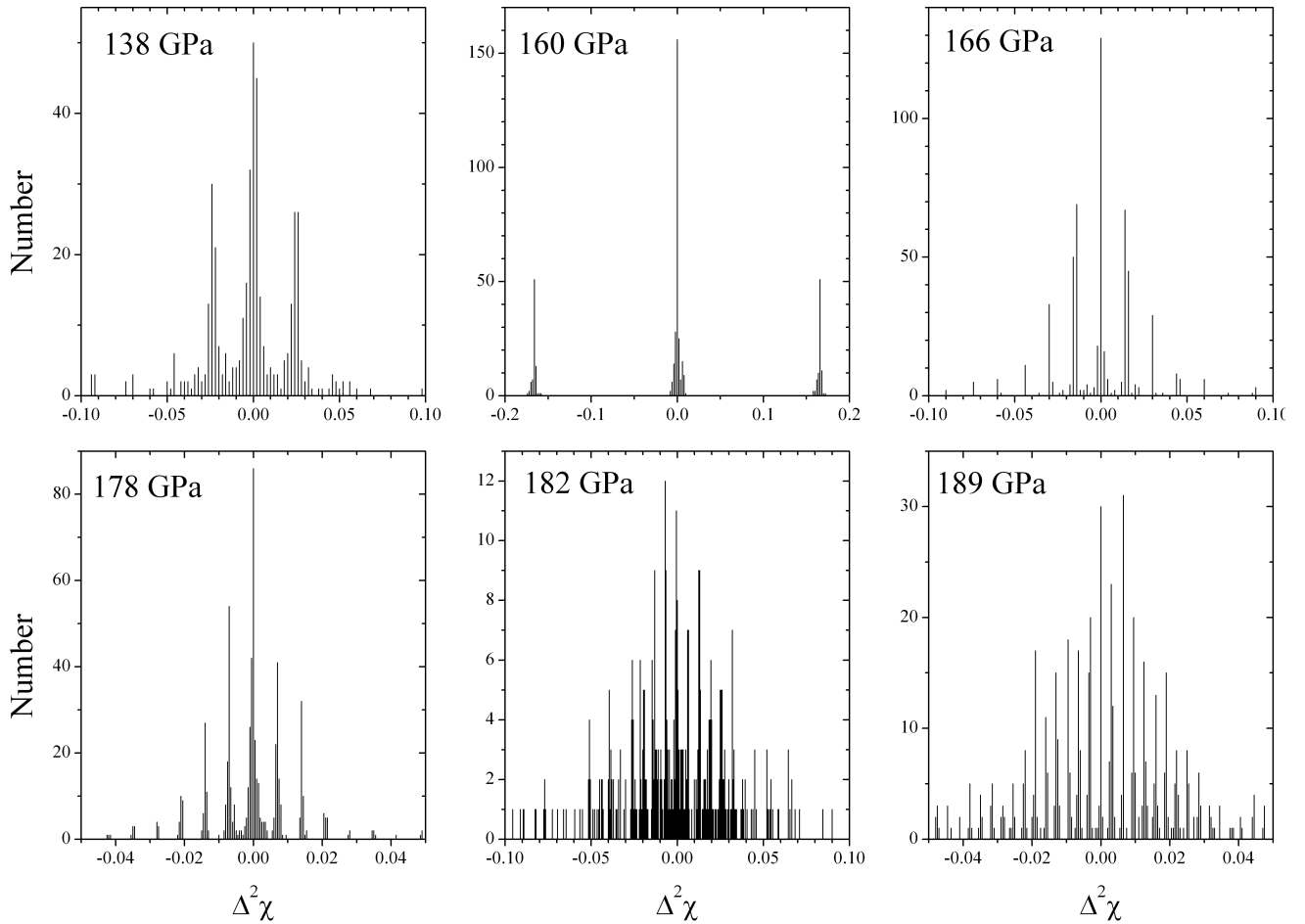


FIG. 11. Histograms of $\Delta^2\chi$ of the “superconducting signal” at all pressures. This representation of the data was introduced by Dukwon [14, 15].

(Figs. 11, 17, 18 and 19) are the smallest for 189 GPa. The corresponding quantization values are

- 138 GPa: ~ 0.025 nV
- 160 GPa: ~ 0.17 nV
- 166 GPa: ~ 0.016 nV
- 178 GPa: ~ 0.007 nV
- 182 GPa: ~ 0.006 nV
- 189 GPa: ~ 0.003 nV

This suggests that for all pressures the “superconducting signal” is the sum of a quantized component $q(T)$ and a smooth function $s(T)$. In all cases the distribution of $\Delta^2\chi$ has some broadening, and this effect is most important when the step size is smallest.

To understand this, we first note that the sawtooth-like “superconducting signal” or 160 GPa can be easily converted into a curve that looks like the other pressures by a simple adjacent averaging smoothing. For commercial plotting software this smoothing is the most commonly used

option in case the intervals along the x-axis are not equally spaced. The default value is averaging over 5 points. Applying this to the 160 GPa “superconducting signal” gives the results shown in Figs. 20, 21 where the unsmoothed susceptibility and its first and second derivative is compared to the results after 5-point, 9-point and 19-point adjacent averaging. In Fig. 15 the corresponding histograms are shown. One observes that

1. The quantization step Δ_q is equal to the step-size Δ_0 of the unsmoothed data divided by the number n of adjacent averaging points: $\Delta_q = \Delta_0/n$.
2. On the scale of the quantized steps the straight segments in the second derivative become progressively meandering when the number of averaging points is increased. In the corresponding histograms this shows up as progressive broadening of the peaks.
3. Long third order polynomial segments, such as the one in the region around 168 Kelvin, disappear when the number of averaging points exceeds the length of the polynomial segment, in this case for 19 point

adjacent averaging as shown in the bottom panel of 21.

To check whether these considerations apply to the measurements at all pressures, we take a closer look at Figs. 17, 18, 19. For 138, 160 and 178 GPa numerous smooth sections show up prominently in the first derivative. For 166 GPa curved smooth sections in the first derivative are present below T_c , for 178 GPa above T_c . All in all it looks similar to the simulation in Figs. 20, 21 where in regions with a high density of quantized steps, the polynomial sections become blurred because the adjacent averaging merges them with neighboring sections. At the same time the quantization effect is *not* removed by adjacent averaging, instead it shows up as aliasing in the first and second derivatives with step-size $\Delta_q = \Delta_0/n$. If the quantized component is superimposed on a function containing random noise $\delta s(T)$, the aliasing effect disappears for n large enough so that $\Delta_q < \delta s(T)$. The aliasing effect in $\Delta^2\chi$ in Figs. 17, 18, 19 demonstrates that for all pressures the “superconducting signal” is a superposition of a quantized component $q(T)$ and a smooth function $s(T)$, *i.e.* noise -if present- has smaller amplitude than the step-size.

Summary of “superconducting signal” at all pressures

- For all pressures the “superconducting signal” is the superposition of a quantized component and a smooth component. For the 160 GPa data the smooth component is a 15 point cubic spline with normal boundary conditions.
- For all pressures except 160 GPa an adjacent averaging smoothing has been applied to the “superconducting signal”.

IX. MEASURED VOLTAGE AT ALL PRESSURES

The temperature traces of the “measured voltage” at 160 GPa shown in Fig. 10 and the corresponding histogram of $\Delta^2\chi_{mv}$ displayed in Fig. 16, show clear signatures of the quantized steps in the “measured voltage” reported in [1, 2] at ± 0.2 nV. We have verified that all steps contributing to the maxima at ± 0.2 nV coincide with steps of the “superconducting signal” [17]. For all other pressures smoothing of the “superconducting signal” has strongly reduced the size of the steps. Despite their smaller size, these steps are nonetheless manifested by the aliasing effect in the temperature traces and histograms of $\Delta^2\chi_{sc}$. In the “measured voltage” χ_{mv} the steps are obscured by the larger amplitude of the noise present in the background signal χ_{bg} that, as we will argue below, has been added to χ_{sc} . The exception is 160 GPa, where the steps *do* show up in the “measured voltage” due to the fact that their size (0.17 nV) is much larger than for the other pressures (< 0.025 nV). This difference originates in the fact that, unlike for the other pressures, the “superconducting signal” at 160 GPa is not smoothed.

A simulation is shown in Fig. 22, where for the background signal an arbitrary curve was taken having a noise structure similar to that shown in Fig. 2a of Ref. [12]. (i) The “measured voltage” is noisier than “superconducting signal” and “background signal” and (ii) several (but not all) of the steps present in the “superconducting signal” also show up in “measured voltage”. In the corresponding histogram of $\Delta^2\chi$ (bottom panel of Fig. 22) the peaks due to the quantized steps around ± 0.17 nV remain visible despite the broadening due to the noise of the added “background” signal, just as in Fig. 16 top right panel.

Additional insight is provided from correlations between $\Delta^2\chi_{mv}$ and $\Delta^2\chi_{sc}$. In Figs. 12, 13, 23, 24, 25, 26 correlation maps in the $(\Delta^2\chi_{mv}, \Delta^2\chi_{sc})$ plane are displayed for all pressures. The scale of the maps has been adjusted according to the quantization step size Δ_q deduced from $\Delta^2\chi_{sc}$ (Figs. 11, 17, 18 and 19). For 138, 160, 166, and 178 GPa the steps present in the “superconducting signal” are clearly revealed as vertical stripes. For 138 and 160 GPa the noise in the “measured voltage” is sufficiently small to reveal that $\Delta^2\chi_{mv}$ has the same step structure as $\Delta^2\chi_{sc}$. This shows up in the map for 138 GPa as a pile-up of points around $(-0.025, -0.025)$ and $(0.025, 0.025)$ and in the map for 160 GPa around $(-0.17, -0.17)$ and $(0.17, 0.17)$. In Fig. 14 this is shown in the form of histograms of $\Delta^2\chi_{mv}$ corresponding to the vertical stripes in the corresponding correlations maps.

For 138 GPa the mean average of $\Delta^2\chi_{mv}$ of these distributions correspond to -0.024 ± 0.027 nV, 0.001 ± 0.025 nV and 0.020 ± 0.025 nV when moving from the stripe $\Delta^2\chi_{sc} = -0.025$ nV through $\Delta^2\chi_{sc} = 0$ nV to $\Delta^2\chi_{sc} = 0.025$ nV. For 160 GPa the mean average of $\Delta^2\chi_{mv}$ of these distributions correspond to -0.162 ± 0.076 nV, -0.005 ± 0.077 nV and 0.176 ± 0.080 nV when moving from the stripe $\Delta^2\chi_{sc} = -0.166$ nV through $\Delta^2\chi_{sc} = 0$ nV to $\Delta^2\chi_{sc} = 0.166$ nV. For the other pressures the noise amplitude in $\Delta^2\chi_{mv}$ is too large compared to the step size to display a statistically significant correlation of this type.

X. SUMMARY

We have analyzed in detail the published “superconducting signal” and “measured voltage” for all pressures reported in Refs. [1, 2]. The following protocol is to our knowledge the only scenario compatible with all reported properties of the data.

Protocol

1. A curve $a(T)$ is generated as the sum of a quantized component $q(T)$ and a smooth function $s(T)$: $a(T) = q(T) + s(T)$.
2. The “superconducting signal” $\chi_{sc}(T)$ (alternatively labeled “data”) is generated by smoothing $a(T)$ using the adjacent averaging method. The 160 GPa data are not smoothed, so that in this case $\chi_{sc}(T) = a(T)$.

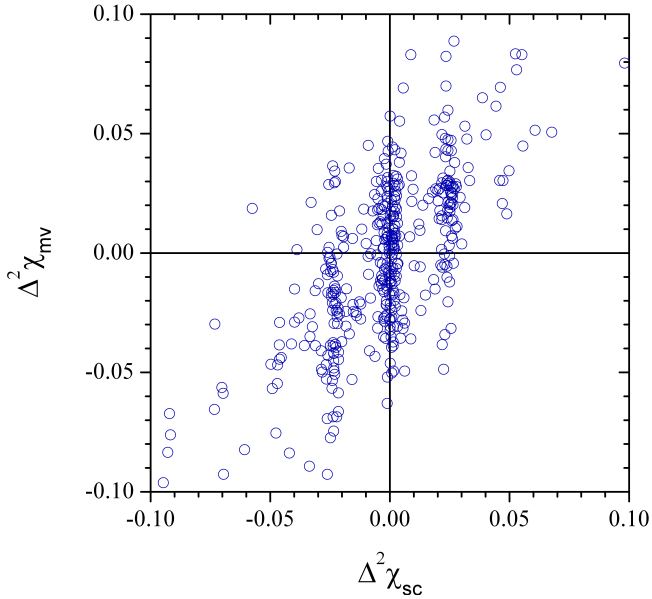


FIG. 12. $\Delta^2\chi_{mv}$ versus $\Delta^2\chi_{sc}$ at 138 GPa.

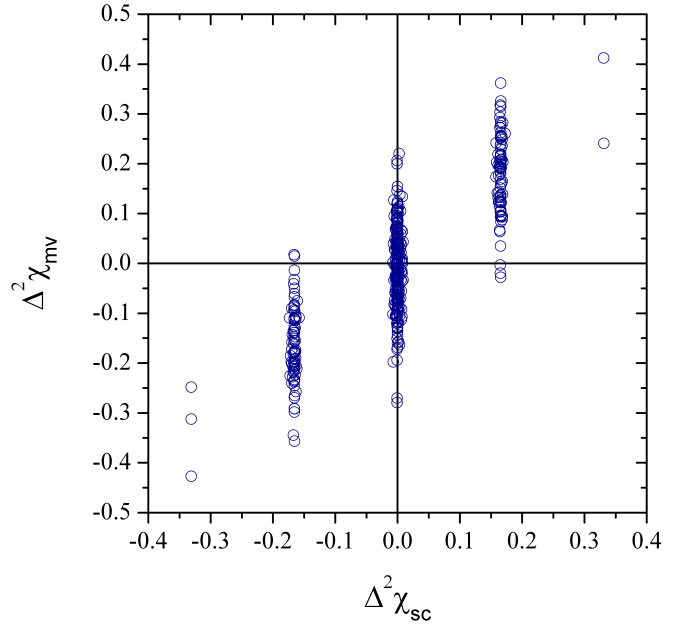


FIG. 13. $\Delta^2\chi_{mv}$ versus $\Delta^2\chi_{sc}$ at 160 GPa.

3. A “background signal” $\chi_{bg}(T)$ is determined and the “measured voltage” $\chi_{mv}(T)$ (alternatively labeled “raw data”) is obtained by adding the “background signal” to the “superconducting signal”: $\chi_{mv}(T) = \chi_{sc}(T) + \chi_{bg}(T)$. In this scenario the noise of “measured voltage” is the sum of the noises of “superconducting signal” and “background signal” and therefore bigger than the noise of each of the latter two.

We have demonstrated that

- For 138, 160, 166, 178, 182 and 189 GPa the “superconducting signal” exhibits the features expected for point 1 of the aforementioned protocol.
- For 160 GPa the smooth function $s(T)$ is a cubic spline with 15 nodes having “normal” boundary conditions at the two extremal nodes, and (ii) $q(T) = \Delta_0 n(T)$ where $\Delta_0 = 0.16555$ nV and $n(T)$ is an integer in the interval $\{-7; 138\}$.
- It is not clear what causes the quantization in increments of 0.16555 nV in the 160 GPa data. The variation as a function of temperature of the “measured voltage” reported in Ref. [2] occurs on a scale ~ 0.0001 nV which is three orders of magnitude below 0.16555 nV.
- The quantized component of the 160 GPa data cannot be identified with the raw data since, other than containing the steep rise at 170 K, it departs strongly from the raw data reported in Ref. [2].
- The multi segment polynomial of the 160 GPa data cannot be identified with the background signal, since it departs strongly from the difference “measured

voltage”-“superconducting signal” according to the data reported in Ref. [2].

- For 138, 166, 178, 182 and 189 GPa the “superconducting signal” exhibits the features expected for point 2 of the protocol.
- For 138 and 160 GPa the “measured voltage” exhibits the features expected for point 3 of the protocol.
- For 166, 178, 182 and 189 GPa point 3 of the protocol can neither be confirmed nor excluded, because in these cases the noise amplitude of $\chi_{bg}(T)$ is too large to allow a statistically significant assessment.

Readers interested to check the analysis resulting in Fig. 1 and Fig. 5 of this paper are welcome to download the corresponding excel tables from Ref. [18, 19]. Numerical data for all pressures reported in Ref. [2] in image format are given in text format in Ref. [16].

ACKNOWLEDGMENTS

We are grateful to Brad Ramshaw, Peter Armitage and Jan Zaanen for stimulating discussions.

XI. SUPPLEMENTARY FIGURES

The figures on the following pages, while referenced in the manuscript, are placed at the end for reasons of layout management.

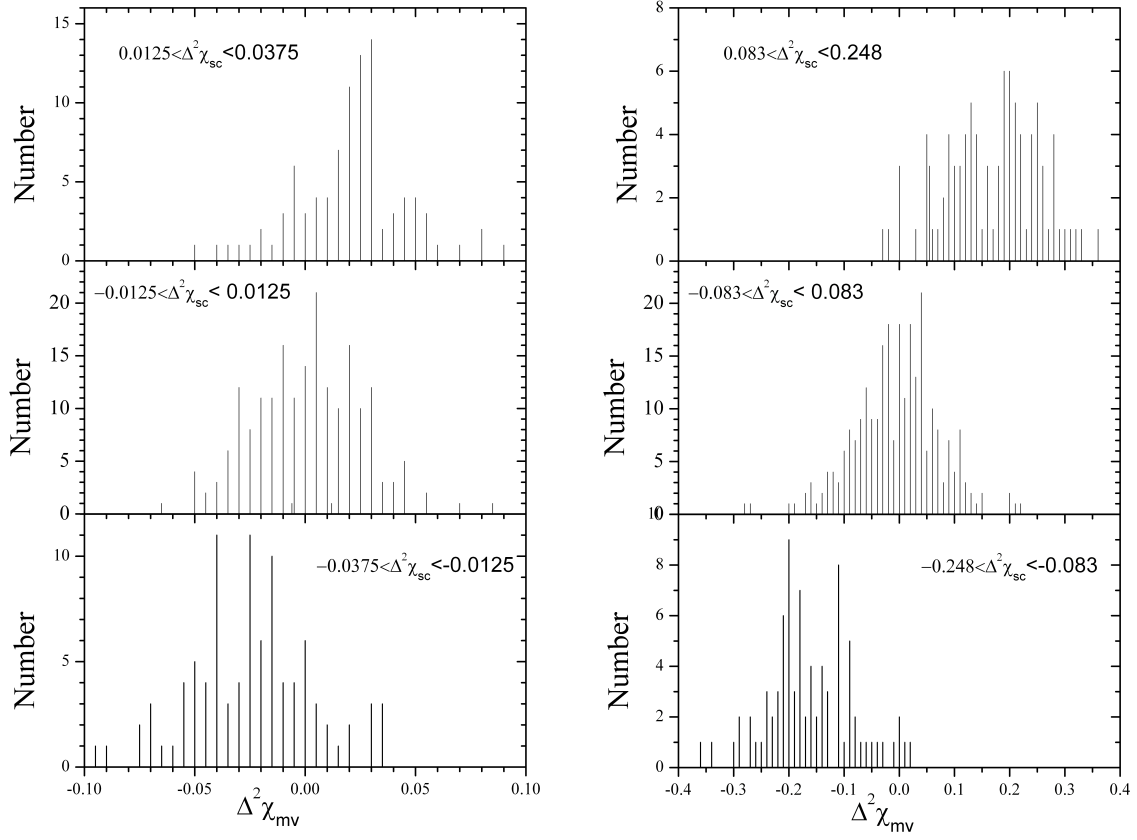


FIG. 14. Histograms of $\Delta^2 \chi_{mv}$ in the slots corresponding to the vertical stripes in Fig. 12 for 138 K and Fig. 13 for 160 K

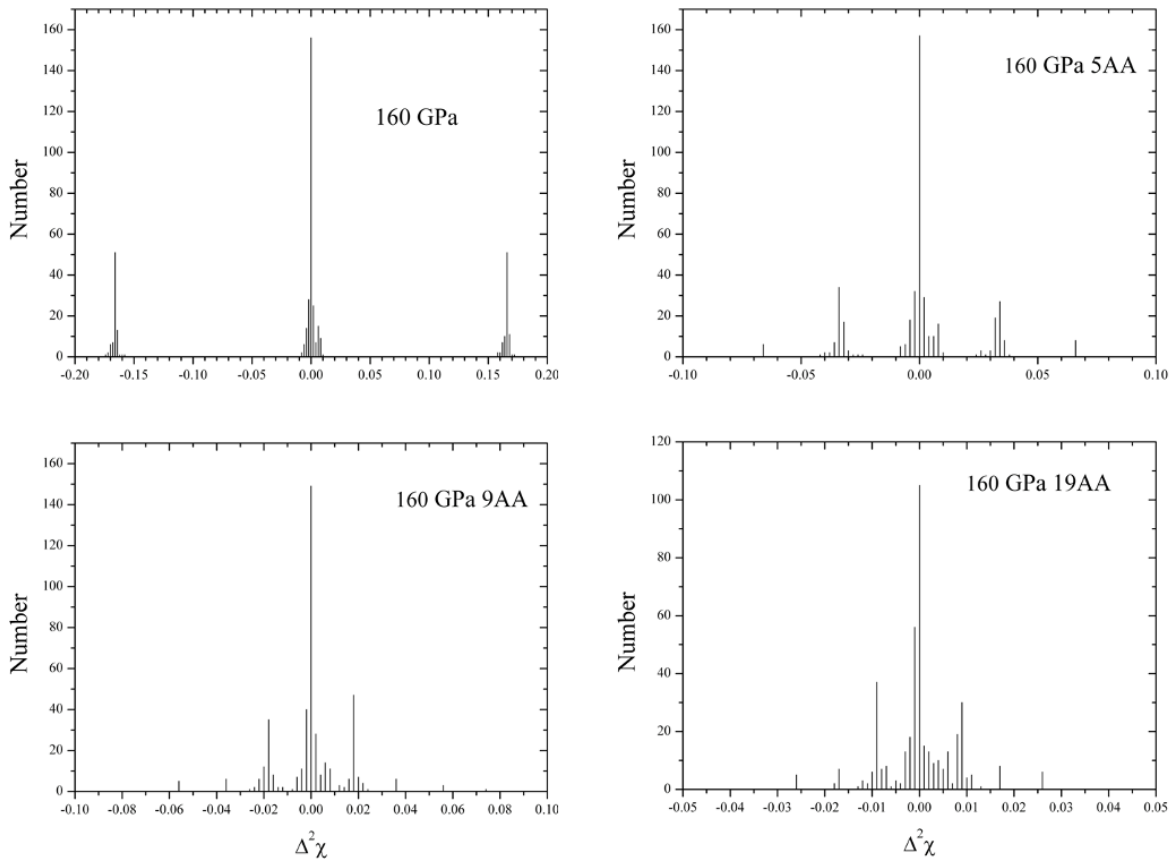


FIG. 15. Histograms of $\Delta^2\chi$ of the “superconducting signal” at 160 GPa, and after 5-point, 9-point and 19-point adjacent averaging.

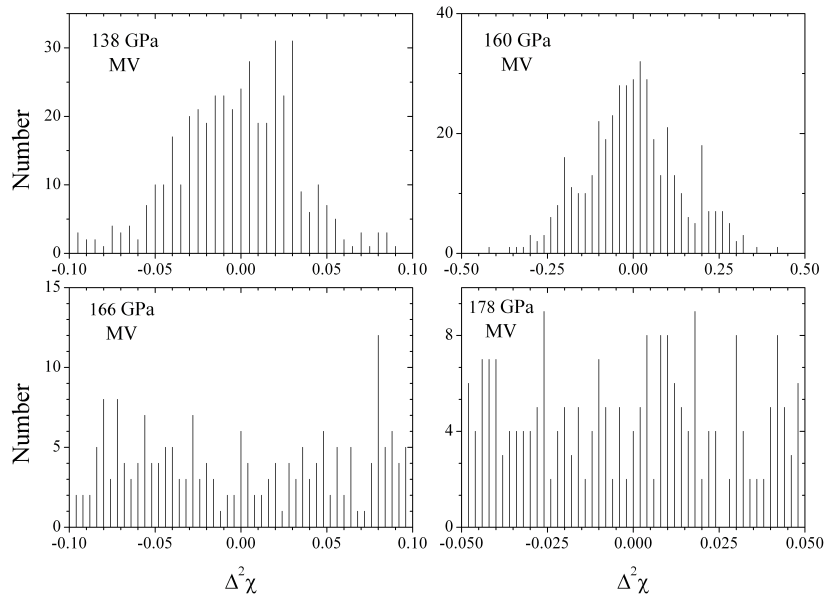


FIG. 16. Histograms of $\Delta^2\chi$ of the “measured voltage” at 138, 160, 166 and 178 GPa. The histograms for 182 and 189 GPa (not shown) are equally featureless as the ones at 166 and 178 GPa.

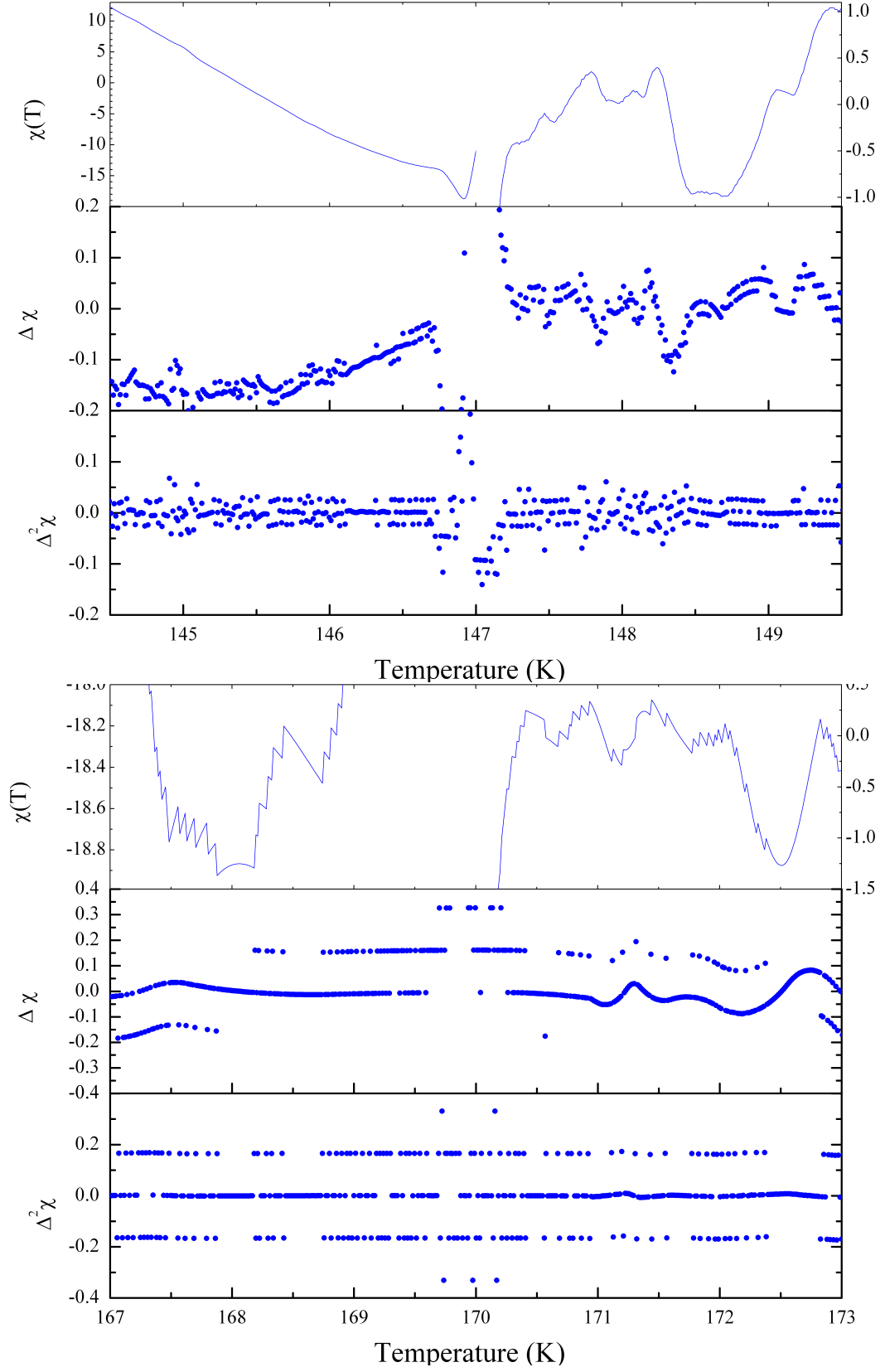


FIG. 17. Superconducting signal $\chi(j)$ for 138 GPa (top) and 160 GPa (bottom), the first discrete differential $\Delta\chi(j) = \chi(j+1) - \chi(j)$ and second discrete differential $\Delta^2\chi(j) = \Delta\chi(j+1) - \Delta\chi(j)$.

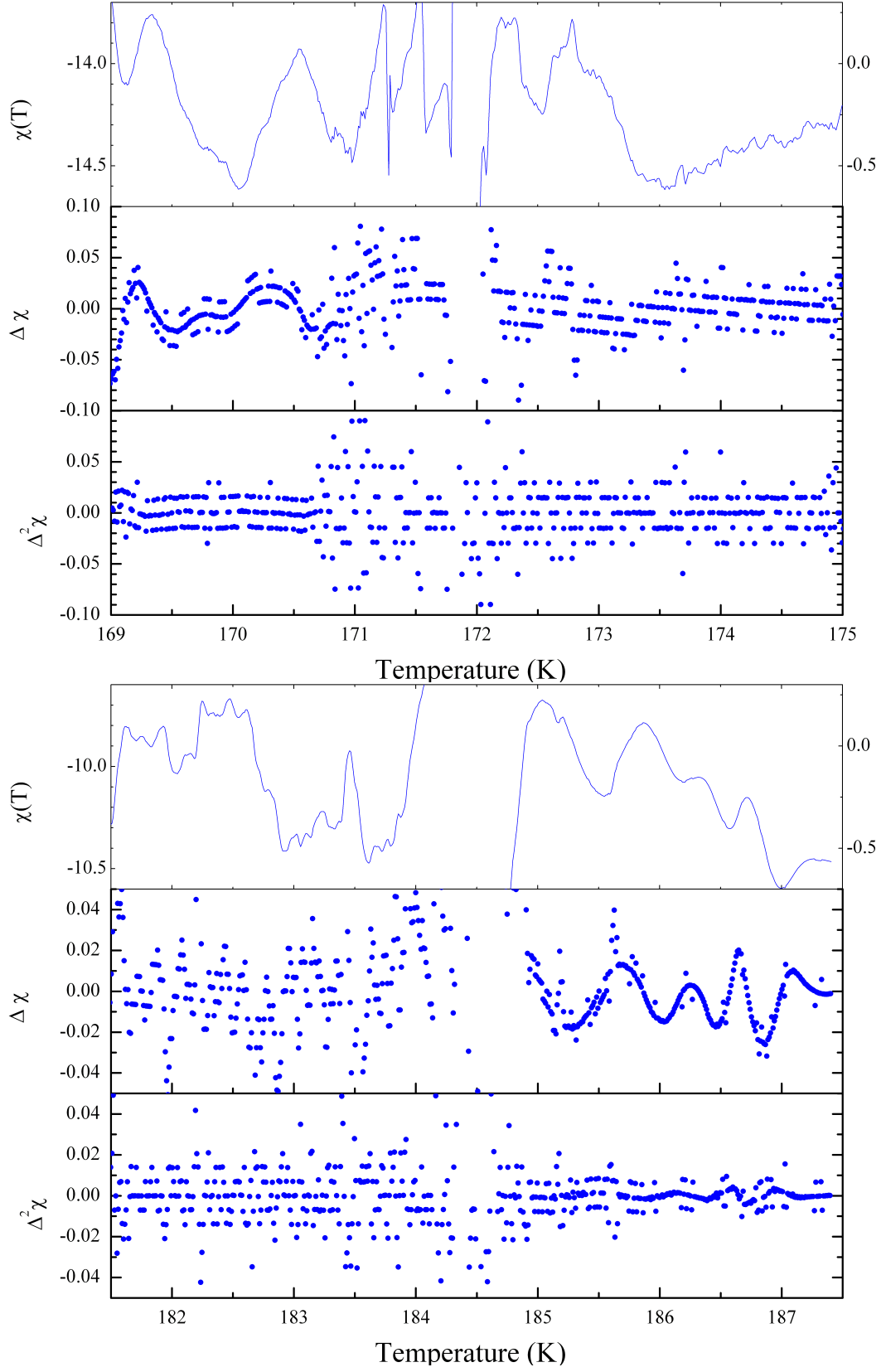


FIG. 18. Superconducting signal $\chi(j)$ for 166 GPa (top) and 178 GPa (bottom), the first discrete differential $\Delta\chi(j) = \chi(j+1) - \chi(j)$ and second discrete differential $\Delta^2\chi(j) = \Delta\chi(j+1) - \Delta\chi(j)$.

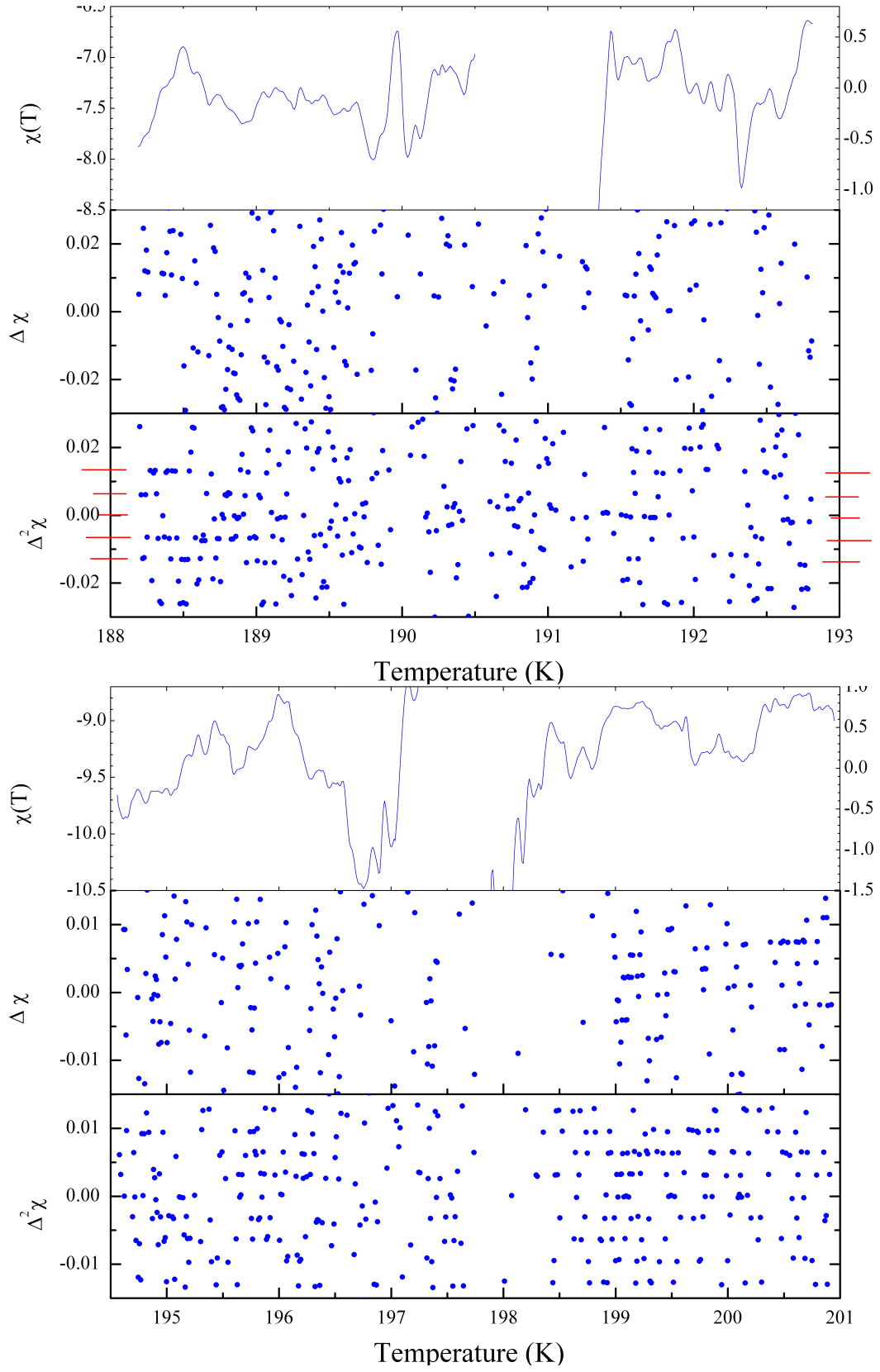


FIG. 19. Superconducting signal $\chi(j)$ for 182 GPa (top) and 189 GPa (bottom), the first discrete differential $\Delta\chi(j) = \chi(j+1) - \chi(j)$ and second discrete differential $\Delta^2\chi(j) = \Delta\chi(j+1) - \Delta\chi(j)$. Since the aliasing effect is less prominent for 182 GPa than for the other pressures, aliasing positions of $\Delta^2\chi$ are marked with red lines.

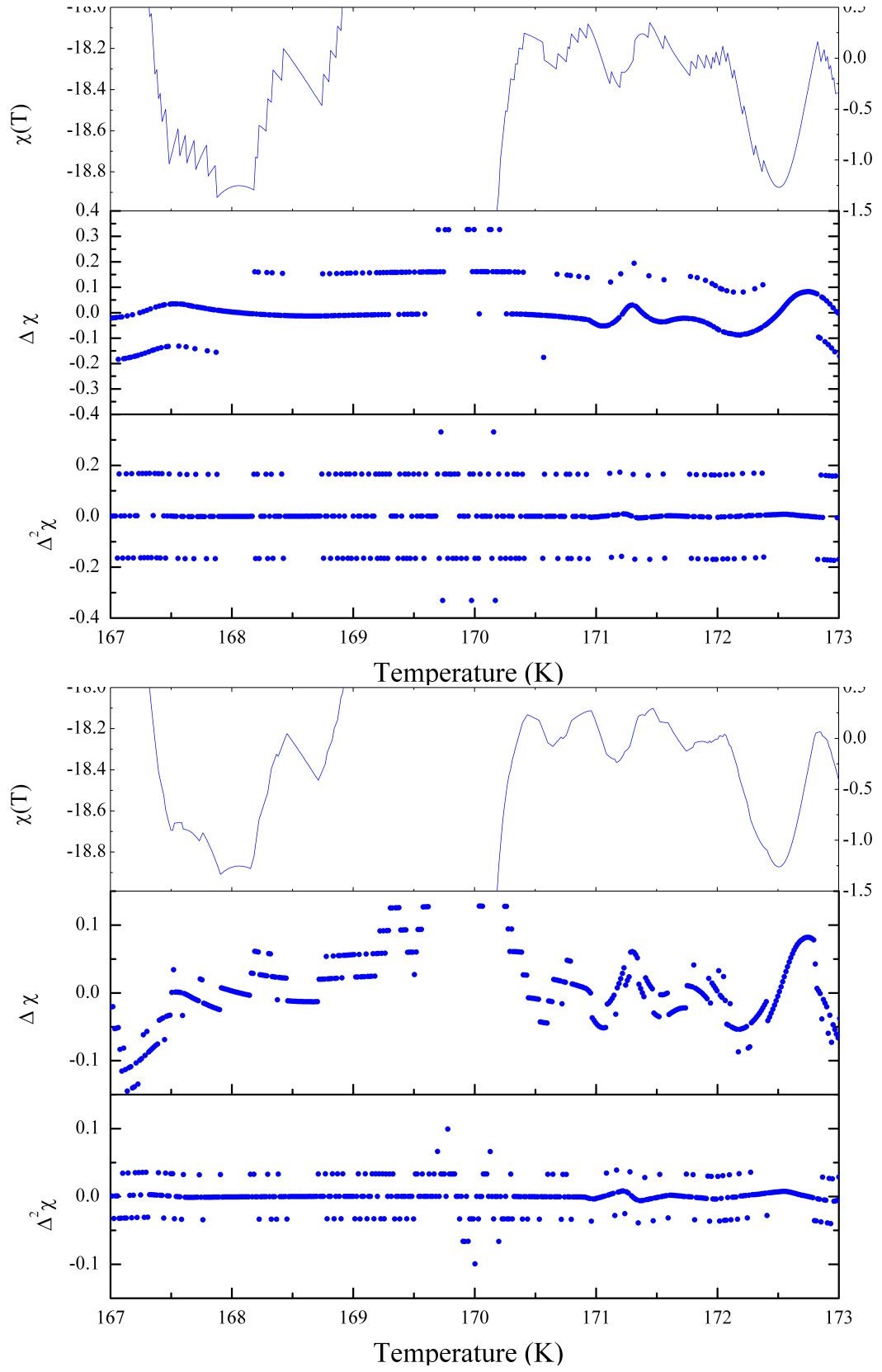


FIG. 20. From top to bottom “superconducting signal” at 160 GPa, the same after 5-point adjacent averaging. For each of these the first derivative is shown in the second row. The second derivative is shown on the third row. Note the closer resemblance with the corresponding quantities for 138 GPa, 166 GPa and 178 GPa (Figs 2 and 3) resulting from the adjacent averaging.

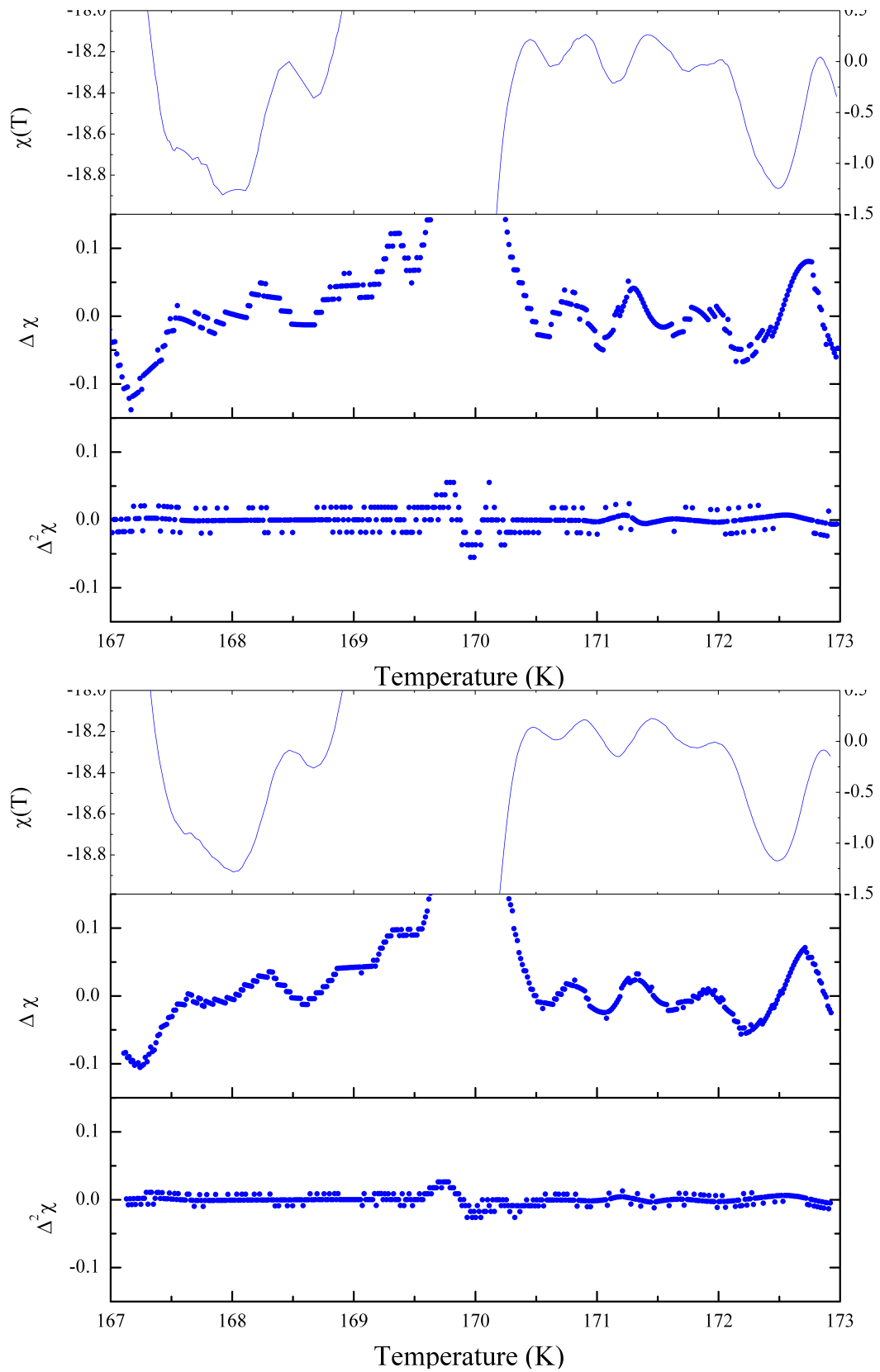


FIG. 21. From top to bottom “superconducting signal” at 160 GPa after 9-point and 19-point adjacent averaging. For each of these the first derivative is shown in the second row. The second derivative is shown on the third row.

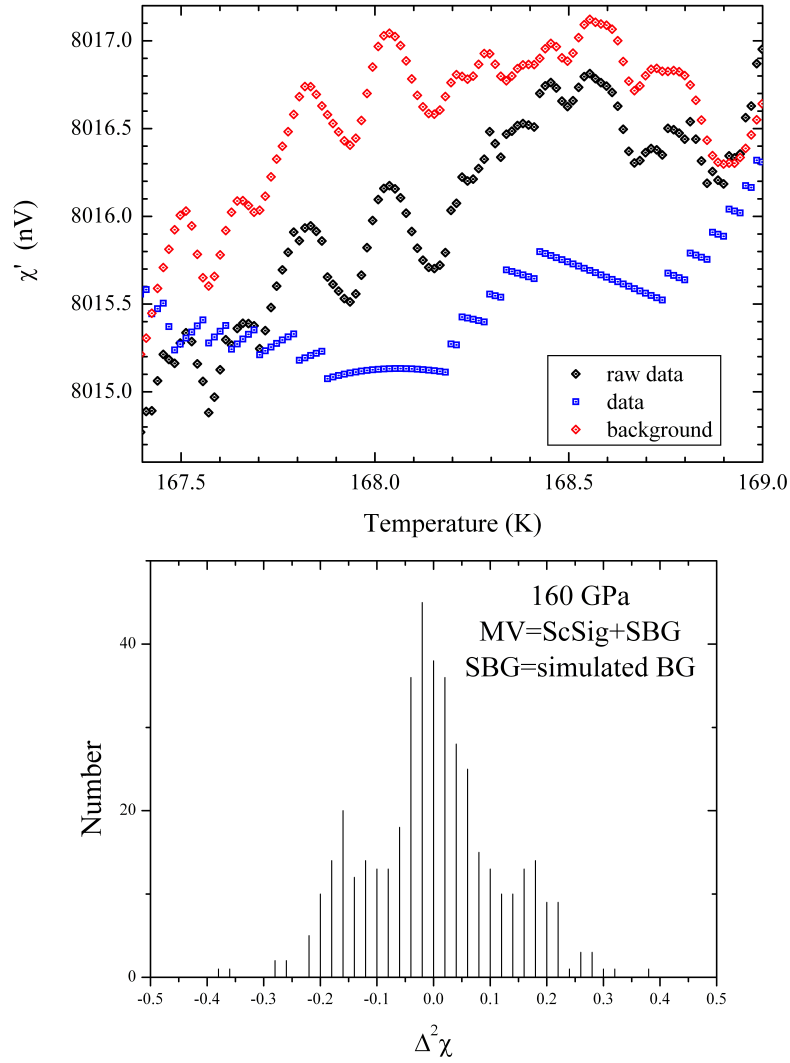
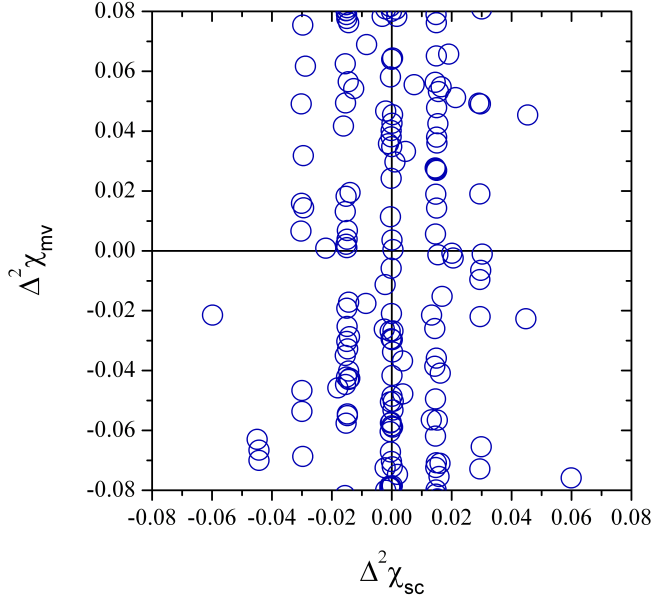
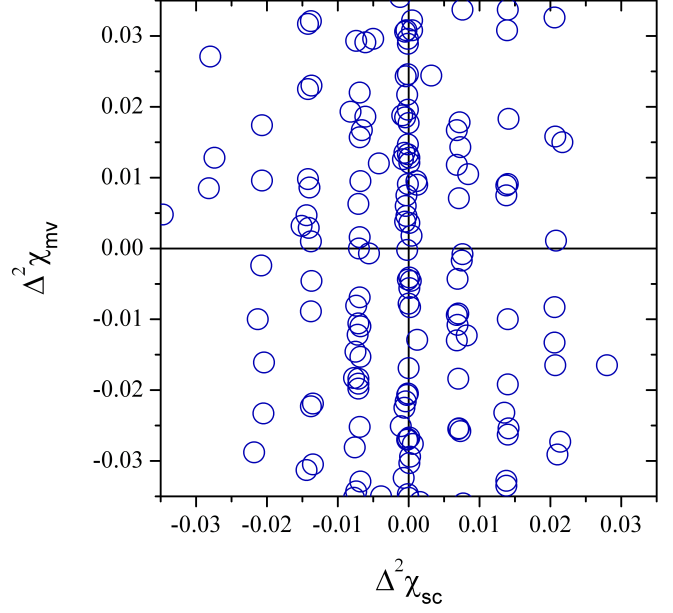
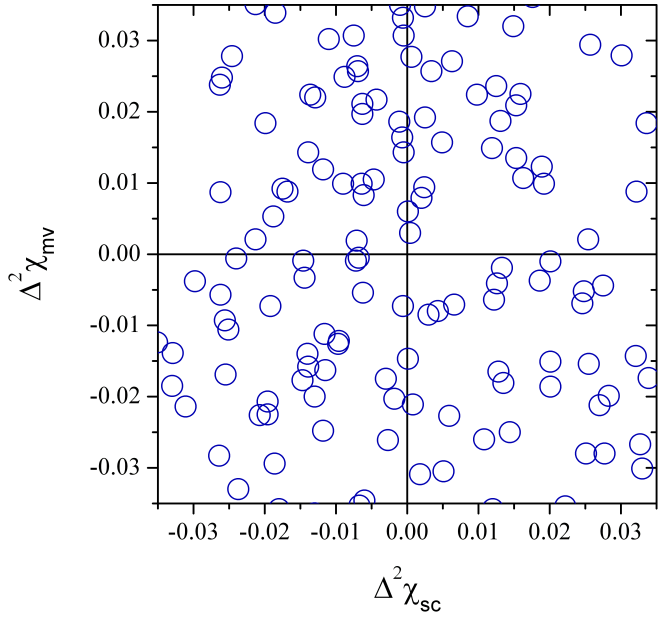
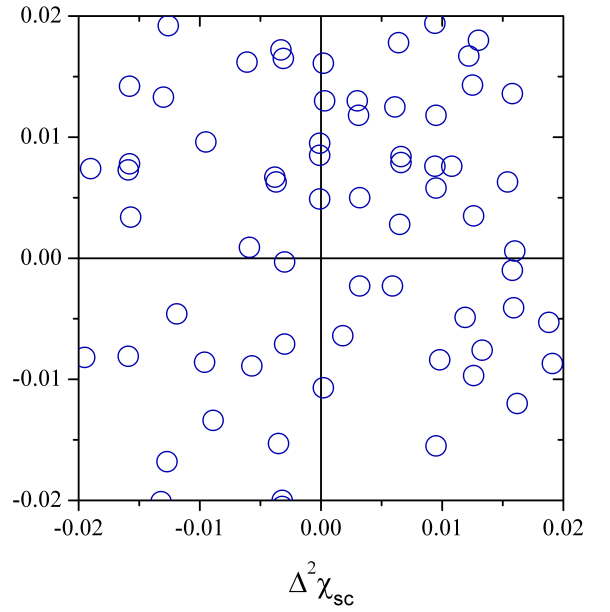


FIG. 22. Top Panel. Blue symbols: “superconducting signal” $\chi_{sc}(T)$ (160 GPa data). Red symbols: “background signal” $\chi_{bg}(T)$ (simulated data). Black symbols: “measured voltage” (alternatively labeled “raw data”) $\chi_{mv}(T) = \chi_{sc}(T) + \chi_{bg}(T)$. Bottom Panel. Histogram of $\Delta^2 \chi_{mv}$.

FIG. 23. $\Delta^2\chi_{mv}$ versus $\Delta^2\chi_{sc}$ at 166 GPa.FIG. 24. $\Delta^2\chi_{mv}$ versus $\Delta^2\chi_{sc}$ at 178 GPa.FIG. 25. $\Delta^2\chi_{mv}$ versus $\Delta^2\chi_{sc}$ at 182 GPa.FIG. 26. $\Delta^2\chi_{mv}$ versus $\Delta^2\chi_{sc}$ at 189 GPa.

- [1] E. Snider, N. Dasenbrock-Gammon, R. McBride, H. Debesai, M.-and Vindana, K. Vencatasamy, K. V. Lawler, A. Salamat, and R. P. Dias, “Room-temperature superconductivity in a carbonaceous sulfur hydride,” *Nature* **586**, 373 (2020).
- [2] R. P. Dias and A. Salamat, “Standard Superconductivity in Carbonaceous Sulfur Hydride,” *arXiv:2111.15017* (Dec. 28, 2021).
- [3] J. E. Hirsch, “Disconnect between published ac magnetic susceptibility of a room temperature superconductor and measured raw data,” *Preprints*, 202112.0115 (2021).
- [4] J. E. Hirsch, “Incompatibility of published ac magnetic susceptibility of a room temperature superconductor with measured raw data,” *Preprints*, 2021120188 (2021).
- [5] Jorge E. Hirsch, “On the room temperature superconductivity of carbonaceous sulfur hydride,” *Europhysics Letters*, DOI:10.1209/0295-5075/ac50c9 (2022).
- [6] Excel files with the quantities shown in Fig. 1 and Fig. 5 are publicly available on Refs. [18] and [19].
- [7] Brad Ramshaw, private communication.
- [8] $y^{(n)}(j) = (S_x S_y - 3S_{xy}) / (S_x^2 - 3S_{xx})$ where $S_x = \sum_{i=j-1}^{j+1} x_i$, $S_y = \sum_{i=j-1}^{j+1} y_i^{(n-1)}$, $S_{xy} = \sum_{i=j-1}^{j+1} x_i y_i^{(n-1)}$, $S_{xx} = \sum_{i=j-1}^{j+1} x_i x_i$.
- [9] “B-spline,” *wikipedia*.
- [10] A cubic spline smoothly connects n nodes with coordinates (x_j, y_j) ($1 \leq j \leq n$) by applying the condition of continuity of first and second derivatives at the $n-2$ internal nodes. Two additional boundary condition are needed to fully define the spline function. Ref. [11] specifies the following types of additional boundary conditions: (i) Natural ($d^2y/dx^2 = 0$ at the two ends), (ii) Not-a-knot (d^3y/dx^3 are continuous for $j = 2$ and $j = N-1$) (iii) Periodic (dy/dx and d^2y/dx^2 are equal for $j = 1$ and $j = N$) (iv) Quadratic (the first and the last segment are quadratic).
- [11] Timo Denk, “Cubic Spline Interpolation,” <https://timodenk.com> (2017).
- [12] R. P. Dias and A. Salamat, “Reply to “Comment on Nature 586, 373 (2020) by E. Snider et al.”,” *arXiv:2201.11883v1* (2022).
- [13] This equation was previously inferred in Ref. [3] from the fact that the noise in the data is significantly smaller than in the raw data.
- [14] Dukwon, “Evidence of..” <https://www.reddit.com> (2022).
- [15] Dukwon, “Histograms of $\Delta^2\chi$,” <https://imgur.com> (2022).
- [16] “Numerical values for all the data given in the tables of Ref. [2],” <https://jorge.physics.ucsd.edu/cshdata.html> (2022).
- [17] The fact that the measured voltage peaks at ± 0.2 nV instead of ± 0.165 nV of the superconducting signal is a statistical fluctuation. To verify this we computed $\sqrt{\langle(\Delta^2\chi_{mv})^2\rangle_{i.s.}}$ for the set of temperatures corresponding to isolated steps in $\chi_{sc}(T)$. The total number of isolated steps is 57. The result is $\sqrt{\langle(\Delta^2\chi_{mv})^2\rangle_{i.s.}} = 0.185 \pm 0.075$ nV. We see that the maximum at ± 0.2 nV falls comfortably within this range of values.
- [18] “Excel files with the quantities shown in Fig. 1,” <http://dirkvandermarel.ch/wp-content/uploads/chi.xlsx> (2022).
- [19] “Excel files with the quantities shown in Fig. 5,” <http://dirkvandermarel.ch/wp-content/uploads/derivchinelv.xlsx> (2022).